

## Evaluating cepharanthine analogues as natural drugs against SARS-CoV-2

**Atsushi Hijikata<sup>1</sup>, Clara Shionyu-Mitsuyama<sup>1</sup>, Setsu Nakae<sup>1</sup>, Masafumi Shionyu<sup>1</sup>, Motonori Ota<sup>2</sup>, Shigehiko Kanaya<sup>3</sup>, Takatsugu Hirokawa<sup>4,5,6</sup>, Shogo Nakajima<sup>7</sup>, Koichi Watashi<sup>7,8,9</sup>, Tsuyoshi Shirai<sup>1,\*</sup>**

<sup>1</sup>Faculty of Bioscience, Nagahama Institute of Bio-Science and Technology, 1266, Tamura-cho, Nagahama, Shiga, 526-0829, Japan

<sup>2</sup>Department of Complex Systems Science, Graduate School of Informatics, Nagoya University, Furo-cho, Chikusa-ku, Nagoya, Aichi 464-8601, Japan

<sup>3</sup>Computational Biology Lab. Division of Information Science, Graduate School of Science and Technology, Nara Institute of Science and Technology (NAIST), 8916-5, Takayama-cho Ikoma, Nara, 630-0192, Japan

<sup>4</sup>Division of Biomedical Science, Faculty of Medicine, University of Tsukuba, Tsukuba 305-8575, Japan

<sup>5</sup>Transborder Medical Research Center, University of Tsukuba, Tsukuba 305-8575, Japan

<sup>6</sup>Cellular and Molecular Biotechnology Research Institute, National Institute of Advanced Industrial Science and Technology, Tokyo 135-0064, Japan

<sup>7</sup>Department of Virology II, National Institute of Infectious Diseases, 1-23-1 Toyama, Shinjuku-ku, Tokyo 162-8640, Japan

<sup>8</sup>Research Center for Drug and Vaccine Development, National Institute of Infectious Diseases, 1-23-1 Toyama, Shinjuku-ku, Tokyo 162-8640, Japan

<sup>9</sup>Department of Applied Biological Sciences, Tokyo University of Science, 2641 Yamazaki, Noda 278-8510, Japan

\*Corresponding author: Tsuyoshi Shirai, Ph.D., Professor

Postal address: Faculty of Bioscience, Nagahama Institute of Bi-Science and Technology, 1266 Tamura-cho, Nagahama, Shiga, 526-0829, Japan.

E-mail: [t\\_shirai@nagahama-i-bio.ac.jp](mailto:t_shirai@nagahama-i-bio.ac.jp)

## **KEYWORDS**

Coronavirus, SARS-CoV, molecular docking, drug repurposing, natural drug

## **ABBREVIATIONS**

ACE2, angiotensin converting enzyme 2; ADV, AutoDock Vina; CEP, cepharanthine; NPC1, Niemann-Pick type C intracellular cholesterol transporter 1; PC, principal component; PCA, principal component analysis; PDB, Protein Data Bank; RBD, receptor binding domain; TET, tetrandrine; TPC2, two pore segment channel 2;

## ABSTRACT

Cepharanthine is a natural biscochlorine alkaloid of plant origin, and recently demonstrated to have anti-SARS-CoV-2 activity. In order to evaluate the other natural analogues as a potential COVID-19 drug, a total of 24 compounds resembling cepharanthine were extracted from the KNApSAcK database, and their binding affinities to supposed target proteins, namely, spike protein and main protease of SARS-CoV-2, NPC1, and TPC2, were predicted *via* molecular docking simulations. Selected analogues were further evaluated by a cell-based SARS-CoV-2 infection assay, and the efficacies of cepharanthine (IC<sub>50</sub> 1.90  $\mu$ M) and tetrandrine (IC<sub>50</sub> 10.37  $\mu$ M) were demonstrated. From a comparison of the docking conformations of these compounds, the diphenyl ester moiety of the molecules was suggested for a putative pharmacophore of the cepharanthine-analogues.

## INTRODUCTION

Despite the successful developments and applications of the COVID-19 vaccines [1,2], considerable numbers of breakthrough infections are still threatening the world health [3,4]. Also, the emergence of novel variants of severe acute respiratory syndrome coronavirus 2 (SARS-CoV-2), which escape from the immunity developed through the vaccinations, is highly concerned [5,6]. These facts should underline the still ongoing requirement of effective anti-SARS-CoV-2 therapeutics.

A part of the authors of the present study recently reported a combined treatment of nelfinavir and cepharanthine (CEP) was highly effective for COVID-19 by screening a panel of the approved drugs in a SARS-CoV-2 cell culture model [7]. Nelfinavir and CEP are the approved drugs for anti-AIDS and anti-leukopenia, respectively. CEP hinders SARS-CoV-2 entry into cells, and nelfinavir inhibited the catalytic activity of viral main protease (M-pro) to suppress viral replication. *In vitro* assay confirmed a synergistic effect of the combined treatment to suppress SARS-CoV-2 proliferation. Nelfinavir was predicted to shorten the period before viral clearance by ~5 days by treatment at early days postinfection, and the additional treatment of CEP enhanced the efficacy significantly.

CEP is a natural product isolated from the plant *Stephania cephalantha Hayata*, and has been approved for leukopenia, xerostomia, and alopecia to date [8]. Natural products like CEP are expected to be promising sources of anti-COVID19 therapeutics [9-12]. It is well known that natural drugs exhibit antiviral activities against notable viral pathogens including coronavirus, dengue virus, coxsackievirus, hepatitis B virus, hepatitis C virus, and influenza virus [13,14]. Therefore, so far, many studies for natural-derived drug discovery have been carried out against SARS-CoV-2 by *in*

*silico* virtual screenings [15-17] as well as *in vitro* assays [18,19]. For instance, quercetin, which is a plant flavonoid and known to have antiviral properties, has been confirmed to block the proteolytic activity of SARS-CoV-2 3CLpro *in vitro* [18], and is currently in a phase 3 clinical trial (ClinicalTrials.gov identifier NCT04578158). The other flavonoids, such as baicalein, herbacetin, and pectolinarin have also been discovered as potent inhibitors for the enzyme [19].

Thus, the efficacies of natural CEP-analogues against COVID-19 would be worth further investigating. In the present study, *in silico* docking study of natural CEP-analogues and a cell-based assay of anti-SARS-CoV-2 activity for selected analogues have been attempted.

## **MATERIALS AND METHODS**

### ***Search for cepharanthine analogues***

The CEP-analogues were sought in the KNApSAcK database [20]. The CEP structure was exhaustively compared with the compounds in the database by using COMPLIG [21]. COMPLIG matches molecular graphs, and evaluates the similarity score of two molecules A and B as  $\min\{M(A, B)/M(A), M(A, B)/M(B)\}$ , where  $M(A)$ ,  $M(B)$ , and  $M(A, B)$  are the total numbers of atoms and bonds in molecules A and B, and the total number of atoms and bonds matched between molecules A and B, respectively. Both element and chirality should be identical for atoms, and bond order should be identical for bonds to be matched, if applicable. A total of 24 compounds with more than 0.90 similarity score were extracted (Table 1). COMPLIG was also used to superimpose the compound structures according to the graph-matching.

### ***Docking study of CEP-analogues and M-pro inhibitors***

The binding affinities of the CEP-analogues and M-pro inhibitors to the receptor binding domain (RBD) of spike protein (S-pro) and M-pro of SARS-CoV-2, Niemann-Pick type C intracellular cholesterol transporter 1 (NPC1), and two pore segment channel 2 (TPC2) of human were predicted *via* molecular docking simulations. The target atom coordinates of S-pro and M-pro were adapted from the previously reported complex models[12] based on the Protein Data Bank (PDB) [22] codes 6m0j [23] and 6lu7 [9], respectively. The NPC1 – NPC2 (NPC intracellular cholesterol transporter 2) complex model was constructed based on PDB code 6w5v [24]. The TPC2 coordinates were based on PDB code 6nq0 [25]. The target coordinates in complex with the best scored CEP are available from <https://harrier.nagahama-i-bio.ac.jp/dtx/SARS-CoV-2/>.

AutoDock Vina (ADV) version 1.0.2 was used to dock the model compounds to the proteins [26]. AutoDockTools version 1.5.6 was used to prepare PDBQT files of the target proteins and compounds [27]. The concaved areas on the protein surface (pockets) were detected using fpocket2 [28]. The pockets overlapping the angiotensin converting enzyme 2 (ACE2) interaction site of S-pro and the active site of M-pro were selected for the target site. For NPC1 and TPC2, preliminary docking simulations of CEP were executed, and two and one pockets, respectively, with the highest docking score were selected for the target sites. The centers of the docking grids (28 x 28 x 28 Å) were defined as the centroid coordinates of amino acid residues composing each pocket (Fig. S2). The size and center of grids were manually modified for S-pro to eliminate the ligands docked outside the ACE2 interacting region (24 x 24 x 24 Å). The docking simulations by ADV were performed with the options exhaustiveness of 1024 and seed of 1024.

The molecular graphics were prepared by using UCSF Chimera [29]. The principal component analysis (PCA) of the docking scores was executed by using the R package [30]. The matrix of the best docking scores of the compounds for SproS, MproS, NPC1S1, NPC1S2, and TPC2S sites (Table 1) was applied to the prcomp function of R with scaling for the PCA. To examine the contribution of each target site/protein to PC axes, the factor loadings (vector of correlation coefficients between the docking score axes and the PC axes) were calculated. The docking scores were sign-inverted so that the factor vectors pointed to the higher-affinity directions.

### ***SARS-CoV-2 infection assay***

The selected compounds for the infection assay experiment were purchased from Adipogen Life Sciences (hesperidin, Cat. No. 83388), Chem Scene LLC (baicalin, CS-5302), Med Chemexpress Co., Ltd (dauricine, HY-N0220; berbamine, HY-N0714), Nacalai Tesque Inc. (tubocurarine, 35637-849), Sigma Aldrich (cepharanthine, SMB00418; hyperoside, 83388), Tim Tec LLC (trilobine, HTS11338), Tokyo Chemical Industry Co., Ltd. (tetrandrine, T3321), and Toronto Research Chemicals Inc. (liensinine, L397833). The anti-SARS-CoV-2 activities of the compounds were assayed in the cell culture model as reported previously [7]. Briefly, VeroE6/TMPRSS2 cells (VeroE6 cells overexpressing transmembrane protease, serine 2 [31]) were inoculated with SARS-CoV-2 Wk-521 strain at an MOI of 0.003 in Dulbecco's modified Eagle's medium (Fujifilm Wako Pure Chemical) supplemented with 10% fetal bovine serum (Sigma Aldrich), 10 units/mL penicillin, 10 mg/mL streptomycin, and 10 mM HEPES pH 7.4 at 37°C in 5% CO<sub>2</sub> for 1 h, and unbound viruses were removed by washing. The compounds were treated in 9 serial dilutions (30.00, 10.00, 3.30, 1.10, 0.36,

and 0.12  $\mu\text{M}$ , and 3 technical replicates were also performed for 5.00, 1.00, and 0.20  $\mu\text{M}$ ) for 24 h and the amounts of extracellular viral RNA were measured. Viral RNA was extracted with a MagMAX Viral/Pathogen II Nucleic Acid Isolation kit (Thermo Fisher Scientific), and quantified by real time RT-PCR analysis with a one-step qRT-PCR kit (THUNDERBIRD Probe One-step qRT-PCR kit, TOYOBO) using the SARS-CoV-2 specific primers and probe [32]. The relative viral RNA levels were calculated by setting that for DMSO control treatment as 1.0 and were plotted against the concentrations of each compound. The cell culture infection assay was handled in a biosafety level 3.

## RESULTS

### *Cepharanthine analogues*

The natural products highly similar to CEP were extracted from the comprehensive species-metabolite relationship database KNApSAcK (Table 1). A total of 24 CEP-analogue compounds showed more than 90% identity in atoms/bonds to CEP by the graph-matching of chemical formula. CEP consists of two coclaurine moieties connected in a cycle. Accordingly, most of the detected analogues were biscoclaurine alkaloids of plant origins. Although the detected analogues largely complied with this molecular architecture of CEP, no one perfectly shared the stereochemistry at two chiral centers and the coclaurine moieties conjugating atom positions with CEP (Fig. S1). It suggested that CEP is a stereochemically unique molecule among the analogues.

Several target proteins have been proposed for the CEP-analogues, such as the spike protein (S-pro) and main protease (M-pro) of corona viruses, Niemann-Pick type C intracellular cholesterol transporter 1 (NPC1), and two pore segment channel 2 (TPC2) of human. However, identities of the target proteins have not been fully confirmed in most of the cases.

CEP is thought to interfere with the ACE2 - S-pro interaction, which is essential for SARS-CoV-2 entry into cells [23], since CEP inhibits the entry phase in viral infection [7]. Also, the interaction of CEP to NPC1 and its efficacy in NPC1 inhibition have been reported [33-35]. NPC1 is the cholesterol transporter, which acts in salvaging cholesterol from the endosomal or lysosomal compartment to the cell membrane. A dysfunction of NPC1 activity results in Niemann-Pick type C disease partly due to a disruption of membrane raft formation, which also works as an obstacle to viral entry into cells [36-38].

Tetrandrine (TET) has been shown to have anti-SARS-CoV-2 activity through inhibiting TPC2 [39]. TPC2 is an endosomal cation channel acts in trafficking LDL molecules, and also known to be involved in viral entry into cells through endosome [40].

M-pro is the most used drug target of SARS-CoV-2, and a few of the CEP-analogues, including curine, are assumed to interact with this enzyme [41]. Therefore, for a comparison purpose, three natural products, which are thought to target M-pro, have also been included in this analysis, namely, baicaline [19], hyperoside [42], and hesperidin [43].

### ***Docking study***

ACE2 interaction site of S-pro RBD (SproS)[23], active site of M-pro (MproS)[9], two putative CEP-binding sites of NPC1 (NPC1S1 and NPC1S2)[24,44], and putative CEP-binding site of TPC2 (TPC2S)[25] were targeted in this study (Figs. 1 and S2).

Docking simulations of the CEP-analogues and the M-pro inhibitors to the hypothetical target sites were performed by using AutoDock Vina [26], and the best score for each pair of compound and target site was evaluated (Table 1). The average score of each compound over the target sites ranged from -8.0 (thalsimine) to -10.2 (kurramine-2'-beta-N-oxide). The average scores for each target site over compounds were -6.7, -9.1, -9.4, -10.8, and -8.1 for SproS, NPC1S1, NPC1S2, TPC2S, and MproS, respectively.

In order to systematically analyze the results of docking simulation, a principal component analysis (PCA) was performed over the matrix of docking scores (Fig. 2). As a result, the cumulative proportion of variance was 86.5% to the second principal component (PC) axis (59.1% and 27.4% for PC1 and PC2, respectively). In the PC1-PC2 plane, the PC1 appeared to mainly represent the affinity of compounds to M-pro and TPC2, and the PC2 separated the compounds by preference between M-pro and TPC2. The viral proteins (S-pro and M-pro) and human proteins (NPC1 and TPC2) were weakly congruent among each group, and CEP seemed to be preferable to the human proteins. The M-pro inhibitors (hyperoside, baicalin, and hesperidin) preferred M-pro, which was consistent with the hypothetical target of the compounds. On the other hand, TET did not show a higher affinity to its supposed target TPC2.

### ***SARS-CoV-2 infection assay***

A total of 10 procurable compounds were selected so that they surround CEP in the PC1-PC2 plane as indicated with coloured circles in Fig. 2, and a cell culture SARS-CoV-2 infection assay was

performed for the compounds. VeroE6/TMPRSS2 cells inoculated with SARS-CoV-2 for 1 h and washed out were incubated with or without the compounds for 24 h and viral RNA in the culture supernatant was quantified (Fig. 3). As a result, CEP was most effective in suppressing viral proliferation ( $IC_{50}$  and  $IC_{90}$  values of 1.90 and 4.46  $\mu$ M, respectively), which was followed by tetrandrine (TET) ( $IC_{50}$  and  $IC_{90}$  values of 10.37 and 14.80  $\mu$ M, respectively). Berbamine, dauricine, and liensinine had even weaker activity to inhibit SARS-CoV-2. Other compounds did not show a significant effect. As a positive control, remdesivir is currently an approved anti-COVID-19 drug directly targeting a SARS-CoV-2 protein with  $IC_{50}$  value of 0.99  $\mu$ M [45].

## DISCUSSION

The natural CEP-analogues have been examined for anti-SARS-CoV-2 activity by combining *in silico* and *in vitro* analyses. The results indicated that CEP showed a potent activity to inhibit SARS-CoV-2 infection among the naturally occurring analogues, which confirmed the previous report [7]. TET was also shown to be effective but had lower activity than CEP. These two compounds are hypothesized to interact with human lysosomal membrane proteins; CEP to NPC1 and TET to TPC2. The natural ligands of these membrane proteins are cholesterol for NPC1 and phosphatidylinositol 3, 5-bisphosphate for TPC2, and consequently the molecular environments of target sites are hydrophobic [24,39]. The CEP-analogues are generally hydrophobic molecules with predicted logP values ranged from 5.8 to 6.7, and those for CEP and TET are 6.5 and 6.4, respectively. Usually, discriminating specificity or evaluating affinity for a highly hydrophobic interaction is difficult. Accordingly, CEP and TET did not localize in the PC1-PC2 plane of the docking scores (Fig. 2), indicating no preference for a particular target was predicted. Thus, the result did not provide additional implications for the target protein of these compounds. CEP and TET are the natural products, and they have neither been designed nor tuned for a specific target protein. It would be probable that they weakly interact with multiple targets, for example NPC1 and TPC2.

Like many of the CEP-analogues, CEP and TET are the cyclic molecules with conjugated coclaurine moieties and their chemical formulas are highly similar. However, due to the difference in configuration at two chiral centers and the positions of the atoms for coclaurine moieties conjugation, the 3D structures of CEP and TET considerably deviated. Therefore, the 3D structures of the best docking-scored CEP and TET and other examined analogues are superimposed to extract common structural features (Fig. 4). The overall structures were not superimposable between the analogues,

including between CEP and TET. The most of the superimposable partial structures to CEP were centered by a diphenyl ester moiety for TET, berbamine, dauricine, and trilobine as indicated with the ball and stick models in Fig. 4. Between CEP and TET, the conformations of the diphenyl ester moiety (meshed in gray for CEP in Fig.4) were similar, and none of the other examined CEP-analogues without remarkable anti-SARS-CoV-2 activity had this CEP-TET structural motif in identical manor. For example, berbamine and duricine took similar conformation at the corresponding parts but lacking methyl group (meshed in magenta for CEP in Fig. 4), which shared between CEP and TET. Trilobine had this methyl group but the conformation of the diphenyl ester moiety was slightly deviated from CEP and TET. The result suggested this common partial structure between CEP and TET as a putative pharmacophore of CEP-analogues.

For the CEP-analogues to be used as anti-COVID-19 therapeutics, their mechanisms of action should be carefully investigated. It has been recently pointed out that the cationic amphiphilic compounds, including CEP, frequently cause cellular phospholipidosis, which is a lysosomal storage disorder characterized by the excessive accumulation of phospholipids. The extents of phospholipidosis were highly correlated with the anti-viral efficacies of the compounds. Such compounds also included hydroxychloroquine, which was initially expected to be an anti-COVID-19 drug, but the clinical trials were, in some cases, terminated partly due to adverse effects [46].

Considering the assumed action mechanisms of CEP and TET, *i.e.*, inhibition of endosomal lipid/steroid trafficking proteins, the same adverse effect would be difficult to be avoided. The drug-induced phospholipidosis is a frequently encountered hindrance in drug development, and recently it becomes clearer that ammonium cation groups in the molecules play a critical role in the symptom [47]. The structural motif suggested for CEP and TET does not contain, though exists close to, the ammonium cations of the molecules, thus it might be useful in designing CEP-derivatives with low adverse effect, for example, replacing ammonium cation without largely affecting the anti-viral efficacies. It might also contribute to further improving CEP or TET to obtain more target specific (to reduce cross reaction) or less specific (to be multi-targeted) drugs.

## **ACKNOWLEDGEMENTS**

This work was partly supported by the Platform Project for Supporting Drug Discovery and Life Science Research (Basis of Supporting Innovative Drug Discovery and Life Science Research (BINDS)) JP21am0101111 and JP21am0101069 to T.S. and the Emerging/Re-emerging Infectious

Diseases Project JP20fk0108411 and JP20fk0108511 to K.W. from The Agency for Medical Research and Development (AMED), and Grants-in-Aid for scientific research from the Ministry of Education, Culture, Sports, Science and Technology-Japan JP19K12211 and JP21H03547 to M.S. and T.S., respectively.

#### **AUTHOR CONTRIBUTIONS**

M.O., S.K., and T.S. conceived and designed the study. A.H., C.S., S.Nakae, M.S., T.H. and T.S. executed the modeling and docking studies. S.Nakajima and K.W. did the infection assay. A.H., C.S., S.Nakae, M.S. and T.S. wrote the manuscript. All authors commented on the manuscript.

#### **DECLARATION OF INTERESTS**

The authors declare no competing interests.

**Table 1. CEP-analogues and M-pro inhibitors**

Name	KNAPSAcK CID	Similarity score	Best docking score for target site					Assay <sup>1</sup>
			SproS	NPC1S1	NPC1S2	TPC2S	MproS	
Cepharanthine	C00001836	1.00	-6.8	-9.5	-9.3	-11.6	-7.9	*
Daphnandrine	C00001843	0.99	-6.6	-8.8	-9.0	-11.7	-7.5	
Trilobamine	C00001844	0.97	-6.5	-9.1	-9.9	-11.4	-8.3	
Oxyacanthine	C00001897	0.97	-6.1	-9.0	-9.1	-11.0	-7.5	
Thalmine	C00001922	0.96	-7.0	-8.9	-8.6	-10.4	-8.6	
<i>O</i> -Methylthalicberine	C00001888	0.96	-6.0	-9.1	-8.9	-9.5	-6.5	
Liensinine	C00028473	0.96	-6.9	-8.0	-8.5	-9.7	-7.9	*
Tetrandrine	C00001919	0.95	-6.6	-8.4	-9.3	-9.3	-7.1	*
Tubocurarine	C00001927	0.95	-6.5	-9.4	-9.1	-11.6	-7.6	*
Trilobine	C00001926	0.95	-7.1	-9.9	-9.9	-12.5	-8.9	*
Isotrilobine	C00025914	0.95	-6.8	-9.4	-9.5	-12.6	-8.4	
Aromoline	C00001811	0.94	-6.6	-9.0	-10.1	-11.2	-7.7	
Pycnamine	C00001909	0.94	-6.4	-9.0	-10.0	-11.5	-7.1	
Dauricine	C00001845	0.94	-7.1	-8.0	-9.6	-9.8	-7.9	*
Magnoline	C00025880	0.94	-6.8	-9.4	-10.6	-10.3	-9.0	
Hypoepestephanine	C00050801	0.94	-6.1	-9.6	-9.4	-10.9	-7.4	
Berbamine	C00001817	0.92	-6.4	-9.0	-10.0	-11.6	-7.2	*
Curine	C00025602	0.92	-7.3	-9.5	-9.2	-10.4	-7.4	
Isochondrodendrine	C00001870	0.92	-6.6	-9.2	-8.6	-10.2	-7.2	
Bebeerine	C00001816	0.92	-6.5	-9.3	-8.9	-11.1	-7.4	
Kurramine-2'-beta-N-oxide	C00051175	0.92	-7.5	-10.1	-10.8	-12.7	-10.4	
Thalsimine	C00001923	0.91	-6.2	-8.4	-9.1	-9.6	-6.9	
Thalicarpine	C00001920	0.91	-6.9	-9.5	-9.0	-9.3	-8.4	
Kurramine-2'-alpha-N-oxide	C00027148	0.91	-7.6	-9.7	-10.1	-12.2	-11.3	
Hyperoside	C00005372	0.69	-7.2	-8.4	-8.1	-9.2	-9.3	*
Baicalin	C00001024	0.66	-7.2	-8.8	-9.1	-9.9	-9.3	*
Hesperidin	C00000970	0.65	-6.6	-9.8	-10.0	-10.9	-9.0	*

<sup>1</sup>The compounds used for assay are indicated with asterisk.

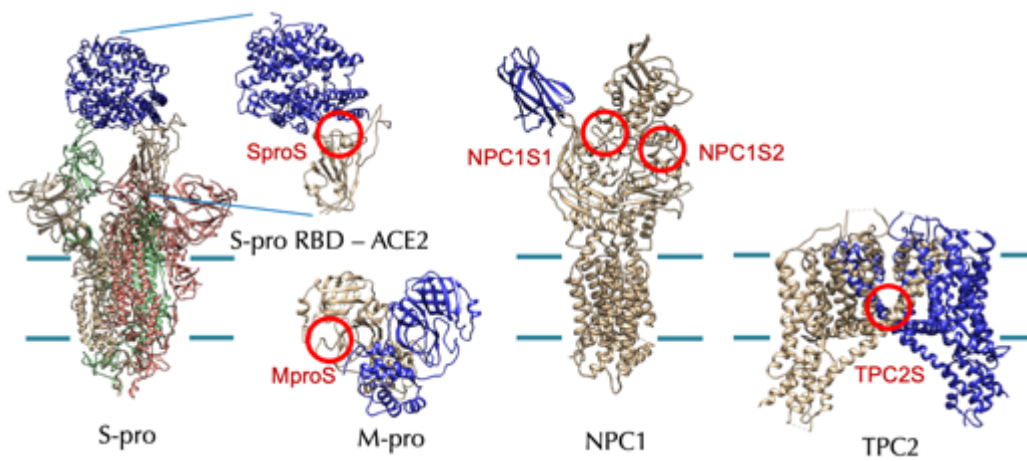


**Fig. 1 Hypothetical target proteins and target sites of CEP-analogues**

The target sites are indicated with red circles. The cell membrane boundaries are shown with green lines for the membrane proteins.

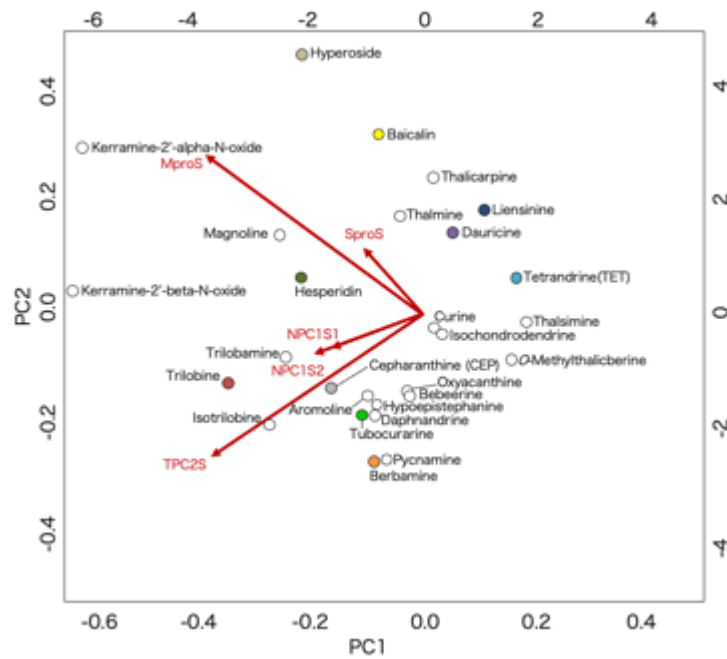


**Fig. 2 Compound distribution in PC1-PC2 plane of docking score**

The compounds are indicated with circles, where those used for assay are differently coloured. The scales on the bottom and left of the plot are the principal component scores of the compounds for the PC1 and PC2 axes, respectively. The loadings of sign-inverted docking scores for the target sites to the principal axes are indicated as overlaid red arrows, and the scales on top and right indicate the corresponding factor loadings. The Figure was prepared by using biplot function of R of default settings and scaling.

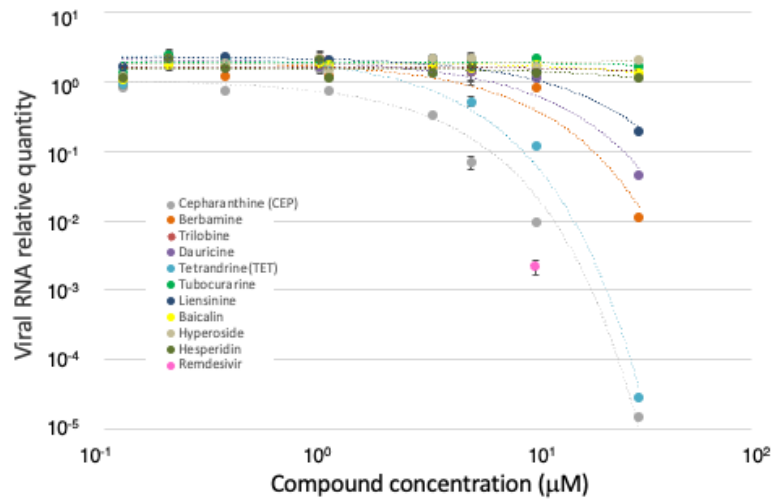


**Fig. 3 Dose-response curves of anti-SARS-CoV-2 activity of compounds**

The relative quantities of secreted viral RNA at 24 h after inoculation (vertical axis in log scale) for all technical replicates are plotted together against compound concentrations (horizontal axis in log scale). The colours for compound plots are coordinated with Fig. 2. The plot in magenta indicates the efficacy of remdesivir at a 10 μM concentration as a positive control.

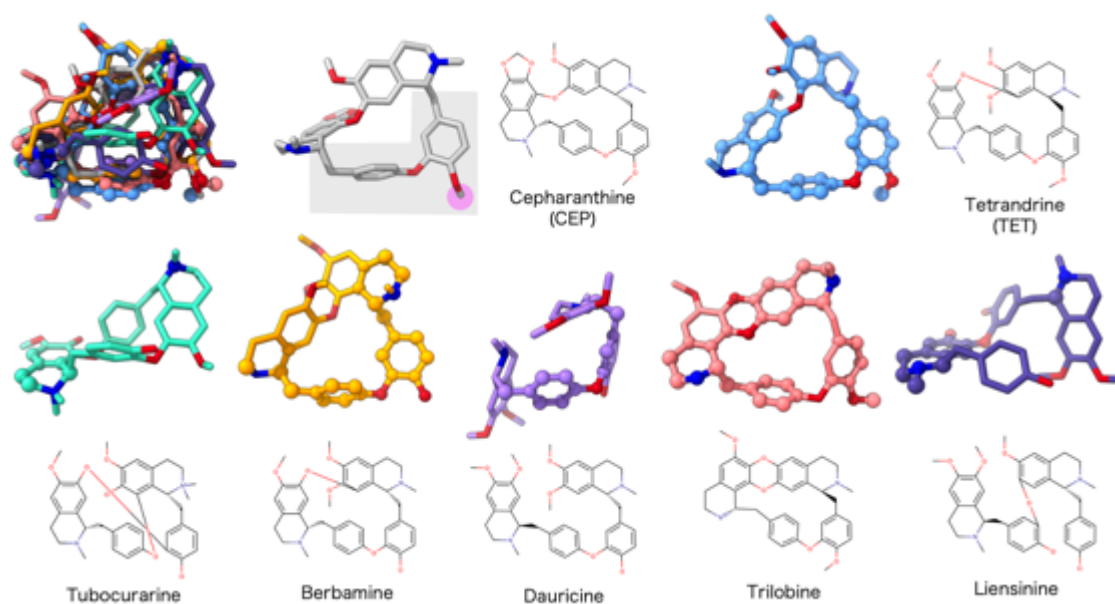


**Fig. 4 Comparison of effective and non-effective CEP-analogues**

3D structures of the CEP-analogues in the best docking-scored conformations were superimposed to that of CEP in the upper left, which is followed by the separate depictions of the same structures. The colours for the models are coordinated with Fig. 2. The atoms within 1.7 Å form the graph-matched atoms of CEP are shown in ball models.

## REFERENCES

- [1] Voysey, M. et al. (2021). Safety and efficacy of the ChAdOx1 nCoV-19 vaccine (AZD1222) against SARS-CoV-2: an interim analysis of four randomised controlled trials in Brazil, South Africa, and the UK. *Lancet* 397, 99-111.
- [2] Baden, L.R. et al. (2021). Efficacy and Safety of the mRNA-1273 SARS-CoV-2 Vaccine. *N Engl J Med* 384, 403-416.
- [3] Team, C.C.-V.B.C.I. (2021). COVID-19 Vaccine Breakthrough Infections Reported to CDC - United States, January 1-April 30, 2021. *MMWR Morb Mortal Wkly Rep* 70, 792-793.
- [4] Brosh-Nissimov, T. et al. (2021). BNT162b2 vaccine breakthrough: clinical characteristics of 152 fully vaccinated hospitalized COVID-19 patients in Israel. *Clin Microbiol Infect*
- [5] Plante, J.A. et al. (2021). Spike mutation D614G alters SARS-CoV-2 fitness. *Nature* 592, 116-121.
- [6] Gupta, R.K. (2021). Will SARS-CoV-2 variants of concern affect the promise of vaccines? *Nat Rev Immunol* 21, 340-341.
- [7] Ohashi, H. et al. (2021). Potential anti-COVID-19 agents, cepharanthine and nelfinavir, and their usage for combination treatment. *iScience* 24, 102367.
- [8] Bailly, C. (2019). Cepharanthine: An update of its mode of action, pharmacological properties and medical applications. *Phytomedicine* 62, 152956.
- [9] Jin, Z. et al. (2020). Structure of M(pro) from SARS-CoV-2 and discovery of its inhibitors. *Nature* 582, 289-293.
- [10] Su, H.X. et al. (2020). Anti-SARS-CoV-2 activities in vitro of Shuanghuanglian preparations and bioactive ingredients. *Acta Pharmacol Sin* 41, 1167-1177.
- [11] Rogosnitzky, M., Okediji, P. and Koman, I. (2020). Cepharanthine: a review of the antiviral potential of a Japanese-approved alopecia drug in COVID-19. *Pharmacol Rep* 72, 1509-1516.
- [12] Hijikata, A., Shionyu-Mitsuyama, C., Nakae, S., Shionyu, M., Ota, M., Kanaya, S. and Shirai, T. (2020). Knowledge-based structural models of SARS-CoV-2 proteins and their complexes with potential drugs. *FEBS Letters* 594, 1960-1973.
- [13] Lin, L.T., Hsu, W.C. and Lin, C.C. (2014). Antiviral natural products and herbal medicines. *J Tradit Complement Med* 4, 24-35.
- [14] Mani, J.S., Johnson, J.B., Steel, J.C., Broszczak, D.A., Neilsen, P.M., Walsh, K.B. and Naiker, M. (2020). Natural product-derived phytochemicals as potential agents against coronaviruses: A review. *Virus Res* 284, 197989.
- [15] Joshi, T., Joshi, T., Sharma, P., Mathpal, S., Pundir, H., Bhatt, V. and Chandra, S. (2020). In silico screening of natural compounds against COVID-19 by targeting Mpro and ACE2 using molecular docking. *Eur Rev Med Pharmacol Sci* 24, 4529-4536.

- [16] Motwalli, O. and Alazmi, M. (2021). Analysis of natural compounds against the activity of SARS-CoV-2 NSP15 protein towards an effective treatment against COVID-19: a theoretical and computational biology approach. *J Mol Model* 27, 160.
- [17] Gani, M.A., Nurhan, A.D., Maulana, S., Siswodihardjo, S., Shinta, D.W. and Khotib, J. (2021). Structure-based virtual screening of bioactive compounds from Indonesian medical plants against severe acute respiratory syndrome coronavirus-2. *J Adv Pharm Technol Res* 12, 120-126.
- [18] Abian, O., Ortega-Alarcon, D., Jimenez-Alesanco, A., Ceballos-Laita, L., Vega, S., Reyburn, H.T., Rizzuti, B. and Velazquez-Campoy, A. (2020). Structural stability of SARS-CoV-2 3CLpro and identification of quercetin as an inhibitor by experimental screening. *Int J Biol Macromol* 164, 1693-1703.
- [19] Jo, S., Kim, S., Kim, D.Y., Kim, M.S. and Shin, D.H. (2020). Flavonoids with inhibitory activity against SARS-CoV-2 3CLpro. *J Enzyme Inhib Med Chem* 35, 1539-1544.
- [20] Afendi, F.M. et al. (2012). KNApSACk family databases: integrated metabolite-plant species databases for multifaceted plant research. *Plant Cell Physiol* 53, e1.
- [21] Saito, M., Takemura, N. and Shirai, T. (2012). Classification of ligand molecules in PDB with fast heuristic graph match $\ddot{y}$  algorithm COMPLIG. *J Mol Biol* 424, 379-90.
- [22] Berman, H., Henrick, K. and Nakamura, H. (2003). Announcing the worldwide Protein Data Bank. *Nat Struct Biol* 10, 980.
- [23] Lan, J. et al. (2020). Structure of the SARS-CoV-2 spike receptor-binding domain bound to the ACE2 receptor. *Nature* 581, 215-220.
- [24] Qian, H., Wu, X., Du, X., Yao, X., Zhao, X., Lee, J., Yang, H. and Yan, N. (2020). Structural Basis of Low-pH-Dependent Lysosomal Cholesterol Egress by NPC1 and NPC2. *Cell* 182, 98-111 e18.
- [25] She, J., Zeng, W., Guo, J., Chen, Q., Bai, X.C. and Jiang, Y. (2019). Structural mechanisms of phospholipid activation of the human TPC2 channel. *Elife* 8
- [26] Trott, O. and Olson, A.J. (2010). AutoDock Vina: improving the speed and accuracy of docking with a new scoring function, efficient optimization, and multithreading. *J Comput Chem* 31, 455-61.
- [27] Morris, G.M., Huey, R., Lindstrom, W., Sanner, M.F., Belew, R.K., Goodsell, D.S. and Olson, A.J. (2009). AutoDock4 and AutoDockTools4: Automated docking with selective receptor flexibility. *J Comput Chem* 30, 2785-91.
- [28] Le Guilloux, V., Schmidtke, P. and Tuffery, P. (2009). Fpocket: an open source platform for ligand pocket detection. *BMC Bioinformatics* 10, 168.

- [29] Pettersen, E.F., Goddard, T.D., Huang, C.C., Couch, G.S., Greenblatt, D.M., Meng, E.C. and Ferrin, T.E. (2004). UCSF Chimera--a visualization system for exploratory research and analysis. *J Comput Chem* 25, 1605-12.
- [30] Team, R.D.C. (2007). R : A language and environment for statistical computing. R Foundation for Statistical Computing, Vienna, Austria. <http://www.R-project.org>
- [31] Matsuyama, S. et al. (2020). Enhanced isolation of SARS-CoV-2 by TMPRSS2-expressing cells. *Proc Natl Acad Sci U S A* 117, 7001-7003.
- [32] Corman, V.M. et al. (2020). Detection of 2019 novel coronavirus (2019-nCoV) by real-time RT-PCR. *Euro Surveill* 25
- [33] Lyu, J. et al. (2017). Pharmacological blockade of cholesterol trafficking by cepharanthine in endothelial cells suppresses angiogenesis and tumor growth. *Cancer Lett* 409, 91-103.
- [34] Sturley, S.L., Rajakumar, T., Hammond, N., Higaki, K., Marka, Z., Marka, S. and Munkacsi, A.B. (2020). Potential COVID-19 therapeutics from a rare disease: weaponizing lipid dysregulation to combat viral infectivity. *J Lipid Res* 61, 972-982.
- [35] Ballout, R.A., Sviridov, D., Bukrinsky, M.I. and Remaley, A.T. (2020). The lysosome: A potential juncture between SARS-CoV-2 infectivity and Niemann-Pick disease type C, with therapeutic implications. *FASEB J* 34, 7253-7264.
- [36] Carstea, E.D. et al. (1997). Niemann-Pick C1 disease gene: homology to mediators of cholesterol homeostasis. *Science* 277, 228-31.
- [37] Incardona, J.P. and Eaton, S. (2000). Cholesterol in signal transduction. *Curr Opin Cell Biol* 12, 193-203.
- [38] Tang, Y., Leao, I.C., Coleman, E.M., Broughton, R.S. and Hildreth, J.E. (2009). Deficiency of niemann-pick type C-1 protein impairs release of human immunodeficiency virus type 1 and results in Gag accumulation in late endosomal/lysosomal compartments. *J Virol* 83, 7982-95.
- [39] Riva, L. et al. (2020). Discovery of SARS-CoV-2 antiviral drugs through large-scale compound repurposing. *Nature* 586, 113-119.
- [40] Penny, C.J. et al. (2019). Mining of Ebola virus entry inhibitors identifies approved drugs as two-pore channel pore blockers. *Biochim Biophys Acta Mol Cell Res* 1866, 1151-1161.
- [41] Singh, S. and Florez, H. (2020). Coronavirus disease 2019 drug discovery through molecular docking. *F1000Res* 9, 502.
- [42] Chen, L. et al. (2006). Binding interaction of quercetin-3-beta-galactoside and its synthetic derivatives with SARS-CoV 3CL(pro): structure-activity relationship studies reveal salient pharmacophore features. *Bioorg Med Chem* 14, 8295-306.

- [43] Lin, C.W., Tsai, F.J., Tsai, C.H., Lai, C.C., Wan, L., Ho, T.Y., Hsieh, C.C. and Chao, P.D. (2005). Anti-SARS coronavirus 3C-like protease effects of *Isatis indigotica* root and plant-derived phenolic compounds. *Antiviral Res* 68, 36-42.
- [44] Li, X., Lu, F., Trinh, M.N., Schmiede, P., Seemann, J., Wang, J. and Blobel, G. (2017). 3.3 A structure of Niemann-Pick C1 protein reveals insights into the function of the C-terminal luminal domain in cholesterol transport. *Proc Natl Acad Sci U S A* 114, 9116-9121.
- [45] Pizzorno, A. et al. (2020). In vitro evaluation of antiviral activity of single and combined repurposable drugs against SARS-CoV-2. *Antiviral Res* 181, 104878.
- [46] Abella, B.S. et al. (2021). Efficacy and Safety of Hydroxychloroquine vs Placebo for Pre-exposure SARS-CoV-2 Prophylaxis Among Health Care Workers: A Randomized Clinical Trial. *JAMA Intern Med* 181, 195-202.
- [47] Breiden, B. and Sandhoff, K. (2019). Emerging mechanisms of drug-induced phospholipidosis. *Biol Chem* 401, 31-46.

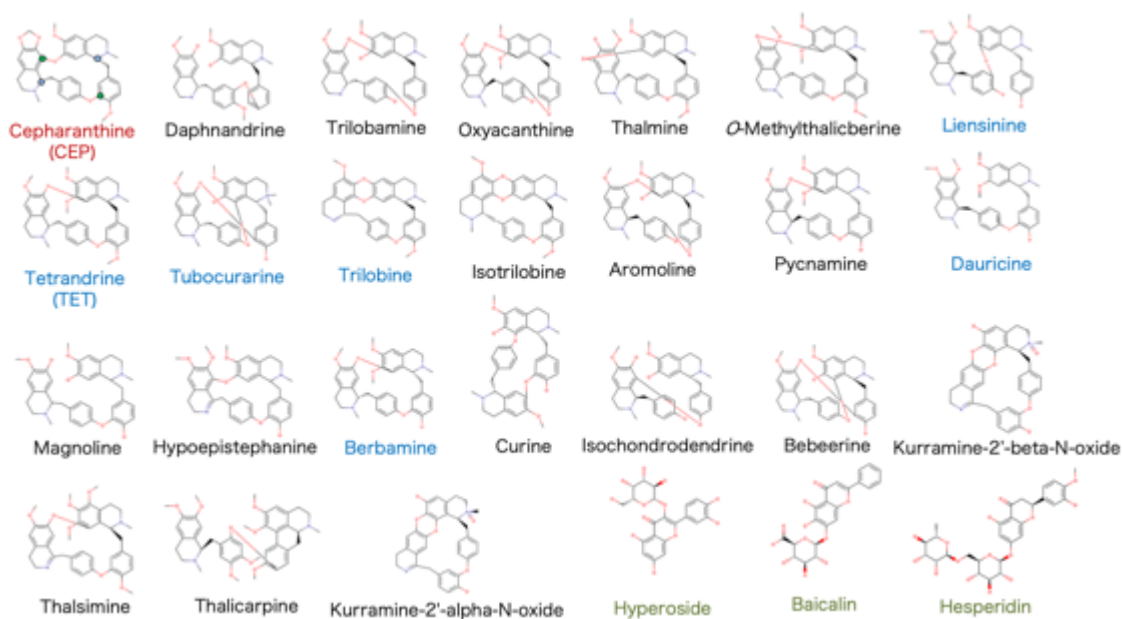


**Fig. S1 Chemical formulas of CEP-analogues and M-pro inhibitors**

The formulas are arranged to be comparable with that of CEP except for the M-pro inhibitors. Two chiral centers and connecting carbon atoms of coclaurine moieties of CEP are indicated with blue and green circles, respectively. The compound names are shown in red (CEP), blue (assayed CEP-analogues), green (M-pro inhibitors), or black (others).

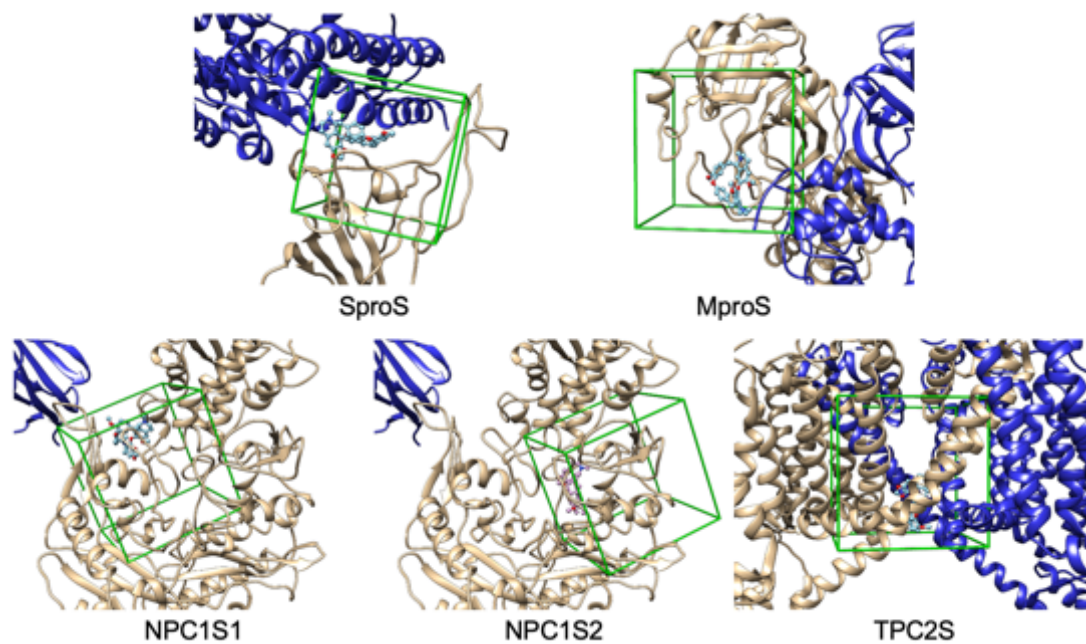


**Fig. S2 Detail of docking sites on target proteins**

The closeup views of the target sites are shown for SproS, MproS, NPC1S1, NPC1S2, and TPC2S. The boxes depicted the search area for the ligands. The best score poses of CEP are shown in ball and stick models for each target site.